Journal of the European Ceramic Society 15 (1995) 929–933

0955-2219(95)00058-5
0955-2219/95/$9.50

Thermal Shock Resistance of $KZr_2P_3O_{12}$–$SrZr_4P_6O_{24}$ Ceramics

Biao Zhang & Jingkun Guo

Shanghai Institute of Ceramics, Chinese Academy of Sciences, Shanghai 200050, People's Republic of China

(Received 29 July 1994; revised 7 March 1995; accepted 10 March 1995)

Abstract

The thermal shock resistance of potassium strontium zirconium phosphate (KSZP) ceramics was investigated by quenching in water. The retained strength of the compositions with very low thermal expansion increased greatly after quenching. These compositions can withstand water quench from 1000°C and still retain their strength before quenching. The relationships between thermal shock resistance and strength, Young's modulus, thermal conductivity, thermal stress, and thermal expansion coefficient was discussed. The thermal shock resistance data measured was compared with that of calculated.

1 Introduction

Materials having high thermal shock resistance are needed for high-temperature applications. Generally, there are two principal ways to design and select materials to achieve high thermal shock resistance.[1] The first way involves the avoidance of fracture initiation, and the second is avoidance of catastrophic crack propagation. A figure of merit for thermal shock resistance is given by

$$R = \sigma/\alpha E \propto \Delta T_c \quad (1)$$

where ΔT_c is the maximum step change in temperature without causing fracture, σ the strength of the material, E Young's modulus and α the thermal expansion coefficient. To avoid fracture initiation by thermal shock, the favorable material characteristics include high strength and thermal conductivity (such as Sialon[2]), and low thermal expansion coefficient (such as LAS glass-ceramic and cordierite ceramic). Most of the structural ceramics have a high Young's modulus and a typical catastrophic decrease in the retained strength. However, to minimize the extent of crack propagation, high Young's modulus and low strength are required. These requirements of Young's modulus and strength are just opposite to those necessary for preventing crack initiation.[3] Hence, the microstructures that exhibit both high thermal shock resistance and high thermal shock damage resistance must be carefully designed. In this respect, ceramics with fine grain size, no defects on grain boundary and small porosity (homogenously distributed) are needed for obtaining high thermal shock resistance. In the case of aluminum titanate,[4] Si_3N_4–BN composite,[5] and Y–TZP,[6] low thermal expansion, microcrack, and large grain size are responsible respectively for their high thermal shock damage resistance. High anisotropic expansion induced microcracks at grain boundaries can restrain crack propagation caused by thermal shock. The increase of the contribution of the transformation toughening of large grain size Y–TZP prevent the thermal stress fracture. The present study was concentrated on the effects of thermal expansion on the thermal shock resistance of two KSZP compositions, $K_{1/2}Sr_{1/4}Zr_2P_3O_{12}$ and $K_{1/4}Sr_{3/8}Zr_2P_3O_{12}$, with magnesia (MgO) additions of 0–8 wt%.

2 Materials and Experimental

Compositions of KSZP with 0–8 wt% MgO are given in Table 1. The KSZP powders were synthesized through coprecipitation and the ceramics were prepared by pressureless sintering. Details of the preparation procedure were described in previous papers.[7,8] Sintering conditions and selected properties are shown in Table 1.

Thermal shock tests were conducted by measuring the retained bending strength after quenching samples from successively increasing temperatures into water at 0°C. The specimens were 2·5 × 5 × 25 mm in dimension. The strength and Young's modulus were measured by three point bending over a 20 mm span at a cross-head speed of 0·5 mm/min (Instron 1195). Each number is the mean

Table 1. Compositions and properties of KSZP ceramics

	Composition	*Sintering condition*		*Density*	*Young's modulus*	*Thermal conductivity at 500°C*	*Phases identified*
		T(°C)	*t(h)*	*(g/cm³)*	*(GPa)*	*(W/mK)*	
K2	$K_{1/2}Sr_{1/4}Zr_2P_3O_{12}$	1300	8	3·01		1·43	Single
K2M2	+2% MgO	1200	1	3·20	109	1·64	Single
K2M2H*	+2%MgO	1200	0·5	3·21	138		Single
K2M5	+5%MgO	1150	1	3·22	108	1·56	+ glass
K2M8	+8%MgO	1110	8	3·25	76	1·62	Two phases
K1	$K_{1/4}Sr_{3/8}Zr_2P_3O_{12}$	1350	2	3·11	—	—	Single
K1M2	+2%MgO	1200	8	3·25	95	—	+ glass
K1M5	+5%MgO	1200	2	3·26	79	—	Two phases
K1M8	+8%MgO	1100	8	3·30	84	1·65	Two phases

*Hot pressed.

result over 5 samples with a maximum dispersion of ±15 MPa.

The measurements for bulk thermal expansion were made on rectangular bars (4 × 4 × 50 mm) using a dilatometer (Model 402-3, Netzsch) from room temperature (RT) to 1000°C at a heating rate of 10°C/min.

The stresses of specimens were determined by using X-ray diffraction method[9] at fixed Ψ (Model D/Max-3A). Strains were determined from 142–143° diffraction angle (2θ) using CrKα radiation at $\Psi = 0°$ and $\Psi = 45°$ on a Φ 40 × 2·5 mm specimen. The total residual stresses (σ_s, includes macrostresses and microstresses) were calculated from the simplified equation:

$$\sigma_s = E \cdot \cot\theta \cdot \Delta 2\theta \cdot \pi/((2(1+\nu) \cdot \Delta \sin\Psi \cdot 180) \quad (2)$$

where Ψ the angle between sample surface and diffraction crystal plane, θ the diffraction angle, $\Delta 2\theta$ the difference of diffraction angle when $\Psi = 0°$ and $\Psi = 45°$, E Young's modulus, and ν Poisson's ratio.

Additionally, thermal conductivities were measured by using a laser heat-conductometer and a differential scanning calorimeter (Model DSC-4, Perkin Elmer).

3 Observations and Discussion

Figure 1 shows the flexural strength of the specimens with various compositions after quenching. The initial strength of K2M5 ceramic is retained up to a critical temperature difference ΔT_c (about 600–800°C) where a sudden decrease in the retained strength occurs. Other ceramics exhibit no instantaneous decline in strength prior to what might be interpreted as a ΔT_c, but do exhibit a more gradual reduction because of microcrack initiation and subcritical crack propagation before ΔT_c is reached. For K2M2 the thermal shock behavior is more complicated.

The retained strength of K2M2 increased markedly after thermal shock. A slight increment of retained strength after thermal shock were observed for K1M2, like that of low thermal expansion aluminium titanate ceramic.[10] It is clear that thermal shock predictions based on so many factors are critically dependent upon the accuracy of that data. The remarkable characteristics of K2M2 ceramic is its low thermal expansion and phase transition. Thermal expansion coefficients of KSZP ceramics are indicated in Table 2. K1 series

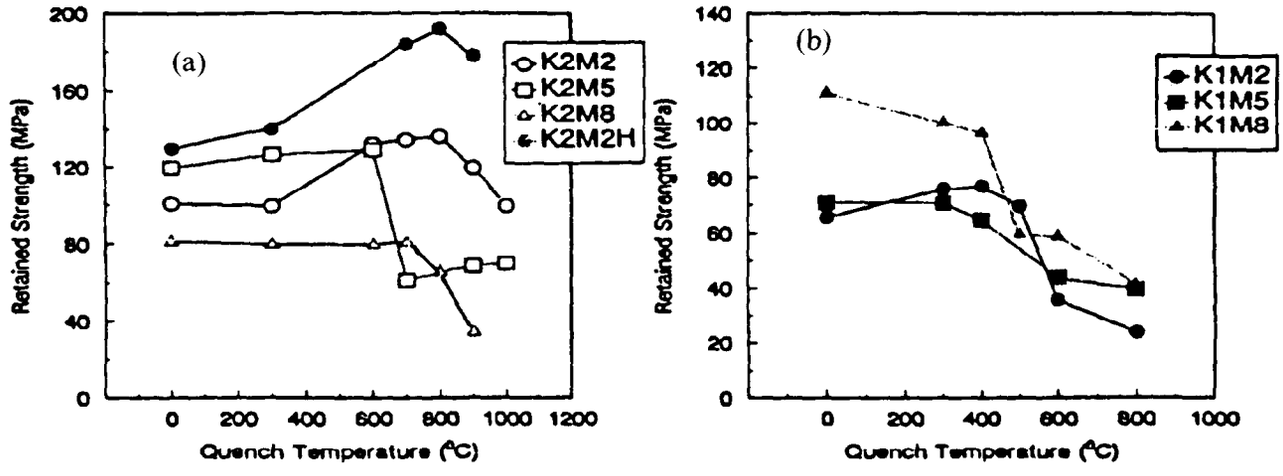

Fig. 1. Thermal shock resistance of (a) K2 series and (b) K1 series of ceramics.

Table 2. Thermal expansion coefficients ($\times 10^{-6}$/°C, RT–T°C) of KSZP ceramics

No.	100 (°C)	200 (°C)	300 (°C)	400 (°C)	500 (°C)	600 (°C)	700 (°C)	800 (°C)	900 (°C)	1000 (°C)
K2	-4·68	-4·16	-3·85	-3·16	-2·23	-1·43	-1·37	-1·44	—	—
K2M2	-1·81	-1·21	-0·55	0·39	1·05	1·19	1·25	1·35	1·46	1·52
K2M2H	-2·38	-1·54	-0·76	-0·25	0·97	1·05	0·75	0·93	1·11	1·72
K2M5	-0·93	-0·35	0·42	0·83	1·08	1·33	1·53	1·79	2·13	2·05
K2M8	-1·41	-1·10	-0·31	0·85	1·24	1·76	2·61	3·53	3·80	3·97
K1	0·21	0·62	0·99	1·30	1·57	1·81	1·92	2·01	—	—
K1M2	1·34	1·65	1·92	2·22	2·43	2·52	2·58	2·68	—	—
K1M5	1·85	2·12	2·44	2·78	2·95	3·03	3·17	3·13	—	—
K1M8	0·77	1·10	2·19	2·39	2·50	2·61	3·05	3·50	4·04	3·24

of ceramics exhibit an overall positive and high thermal expansion, while the thermal expansion coefficients of K2 series of ceramics are low or negative below 300°C. The thermal expansion anisotropy of KSZP is low compared with that of KZP.[8]

To clarify the thermal shock fracture behavior of K2 series ceramics, residual stresses after water quench were measured. The results are shown in Fig. 2. The negative value means compressive stress. The more negative the value, the larger the strength. The stress dependence of quenching temperature stand in direct contrast with each other between K2M2 and K2M5. Compressive stress of K2M2, the lower thermal expansion ceramic, increase with quenching temperature increase and has a sharp change from 300 to 600°C, and is in good agreement with strength variation (Fig. 1(a)). Compressive stress of K2M5, the larger thermal expansion ceramic, decrease with quenching temperature increase, and has a gradual decline. It is also corresponding to its thermal shock result.

Residual stress in single-phase polycrystalline ceramics are of two types: macrostresses and microstresses. Macrostresses generally are near the surface because of differences in processing (such as cutting, grading and quenching) between the surface and the interior. Microstresses arise because grains constrain if the grain is anisotropic. Experimental methods to be used for the determination of residual stress should take into account the two types of residual stress as well as the depth over which the method averages the measurements.[11] A method for separating the macrostresses from the microstresses has been developed by Noyan and Cohen.[12] In this work, the stresses were calculated approximately from eqn (2) as total stresses. Although unable to separate macrostresses from microstresses at these moments, the general trend of stress variation is enough to explain the thermal shock behavior.

As illustrated in Fig. 1(a), the pressureless sintered and hot pressed K2M2 ceramics exhibit similar behavior. Under optical and scanning electron microscope, no obvious cracks were observed. The reason why the significant improvement of residual strength of the K2M2 ceramic after thermal shock is that the ceramic has a very low thermal expansion and phase transition. Below 400°C, the ceramic exhibits negative expansion, whereas above 400°C, it is positive. A phase transformation occurs at 600°C in $K_{1/2}Sr_{1/4}Zr_2P_3O_{12}$ ceramic.[8] The cell volume of the high-temperature phase is larger than that of the low-temperature phase. The phase transition still exists in the K2M2

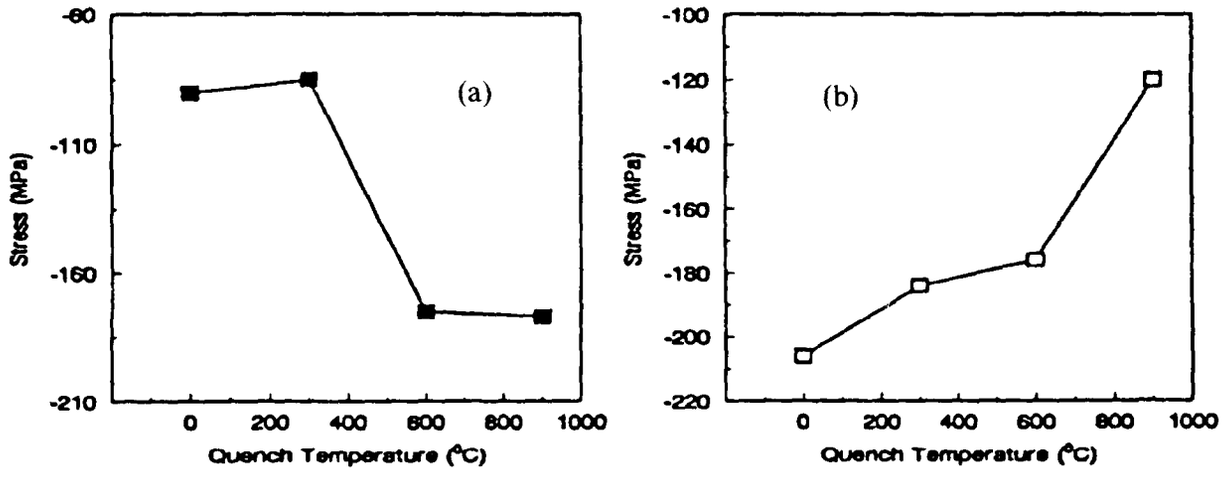

Fig. 2. Total stresses of (a) K2M2 and (b) K2M5 ceramics after water quench from high temperature.

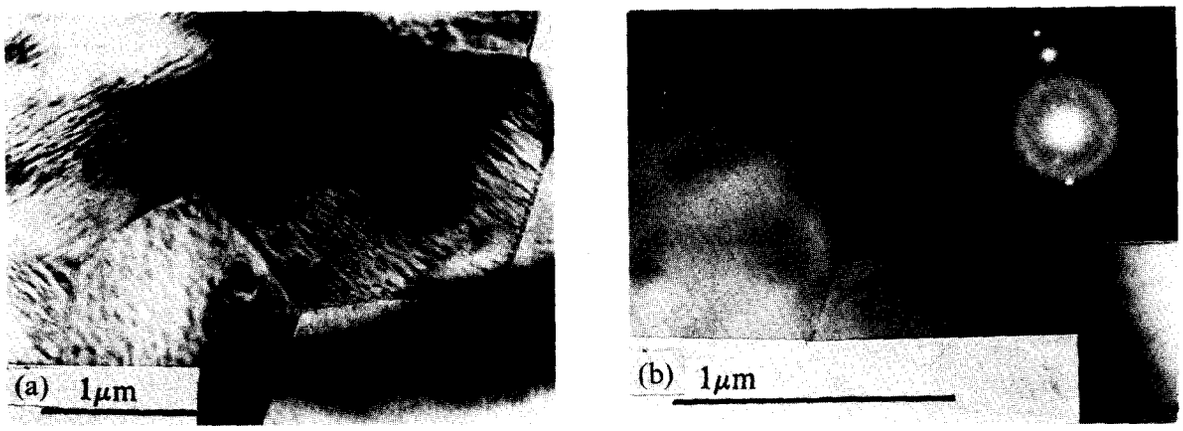

Fig. 3. Microstructure of grain boundaries: (a) bright-field micrograph showing clear boundaries K2M2, and (b) amorphous phase at triple-grain junction and electron diffraction pattern of K2M5 being attached.

ceramic, but it is restrained in K2M5 ceramic. During quenching, the surface region of the specimen cools quickly and shrinks until the temperature reaches 400°C and expands, but the core of the sample cools slowly and still contracts when the surface expands. The surface remains the high-temperature phase and the core transforms to the low-temperature phase. Therefore, the surface is constrained and compressive stresses were formed on the surface. The increment of retained strength occurred just as in strengthened glass. Another reason for high thermal shock resistance of the K2M2 ceramic is no glass phases at the intergranular regions, as suggested by Hoffmann[13] that the ΔT may be connected with the softening of glass phase. TEM micrographs (Fig. 3) show the clear boundaries and junctions of grains for the K2M2 ceramic, but for the K2M5 ceramic, an amorphous phase is observed at triple grain junctions. The residual strength of K2M5 after 1000°C water quenching was a little larger than that of 700°C water quench. This is because that the density of cracks caused by thermal shock increased with increasing ΔT.

For other ceramics, a gradual strength decay is observed. Normally, with most large-grain and large pore ceramics, the retained strength declines slowly when ΔT just exceeds ΔT_c. Relatively, the strength and density of the KSZP ceramics are low and are difficult to sinter, especially for K1 and K2 which have no addition of MgO. For this reason, the thermal shock tests were not conducted on K1 and K2 ceramics.

The application of eqn (1) to KSZP ceramics is shown in Fig. 4(a). The data shows a good fit to eqn (1). Precise theoretical calculations for thermal shock resistance based on material parameters is very difficult. The disagreement between experimental observations and predictions can be attributed to the difference in test methods and inexact property data,[14] especially temperature dependence of mechanical and thermal properties.

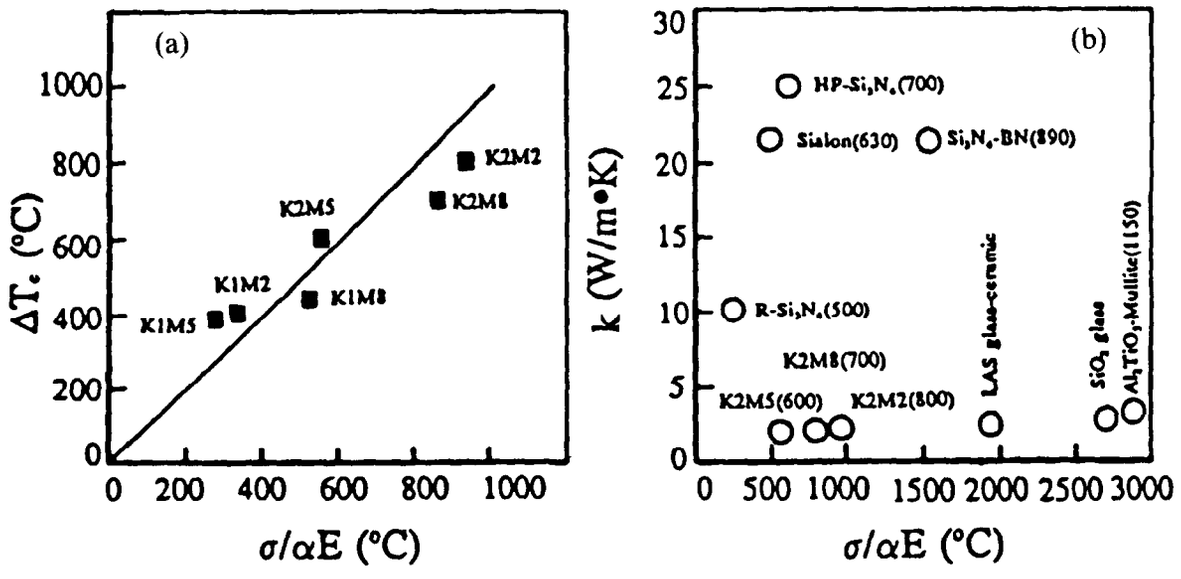

Fig. 4. (a) Thermal shock resistance of KSZP ceramics measured and described in eqn (1), (b) thermal conductivity and thermal shock resistance of SKZP and other ceramics (Refs 2, 5, and 10. The values in parentheses mean ΔT_c).

As is illustrated in Table 2, thermal expansion coefficients, especially low thermal expansion material, are not constant over all the temperature range. They vary significantly in different temperature ranges. It is not clear what an appropriate value for α and σ should be.

Figure 4(b) summarizes the most important properties (k, thermal conductivity, σ, strength, α, the coefficient of thermal expansion, and E Young's modulus) of high thermal shock resistant ceramics. It is indicated that there are two major categories of high ΔT_c ceramics, one with high strength and thermal conductivity, and another with low thermal expansion coefficient. To make an optimum material design and selection of high thermal shock resistant ceramics, guidelines on some factors are needed: high strength, toughness, thermal conductivity, low thermal expansion, less thermal expansion anisotropy resulting in microstructures that can cope with thermal stresses without developing creep cavitation.

4 Conclusions

$KZr_2P_3O_{12}$–$SrZr_4P_6O_{24}$ (0–8 wt% MgO) ceramics possessing low thermal expansion, high thermal shock resistance and high strength have been studied. Thermal expansion coefficients varied in the range of $-4{\cdot}68 \sim 3{\cdot}97 \times 10^{-6}$°C. The thermal shock behavior of low thermal expansion ceramics exhibited some interesting features. The retained strength and compressive stress on the surface of the K2M2 ceramic increased with increasing quench temperature (from 100 MPa at RT to 136 MPa at ΔT = 800°C for pressureless sintered and from 130 MPa at RT to 192 MPa at ΔT = 800°C for hot pressed K2M2 ceramic). The thermal expansion behavior, single phase microstructure, and phase transformation are responsible for its thermal shock behavior. The critical quenching temperature difference varied from 400 to 800°C for KSZP ceramics, which might be used as thermal barrier materials.

References

1. Hasselman, D. P. H., Figures of merit for the thermal stress resistance of high temperature brittle materials: a review. *Ceram. Int.*, **4** (1978) 147–50.
2. Raj, R., Fundamental research in structural ceramics for service near 2000°C. *J. Am. Ceram. Soc.*, **76** (1993) 2147–74.
3. Lutz, E. H., Swain, M. V. & Claussen, N., Thermal shock behavior of duplex ceramics. *J. Am. Ceram. Soc.*, **74** (1991) 19–24.
4. Hamano, K., Ooya, Y. & Kakagawa, Z., Microstructure and mechanical strength of aluminum titanate ceramic prepared from a mixture of aluminum and titania. *Yogyo Kyokaiski*, **91** (1983) 94–101.
5. Sinclair, W. & Simmons, H., Microstructure and thermal shock behavior of BN composites. *J. Mater. Sci. Lett.*, **6** (1987) 627–9.
6. Ishitsuka, M., Sato, T., Endo, T., Shimada, M., Ohno, H., Igawa, N. & Nagasaki, T., Grain-size dependence of thermal shock resistance of yttria-doped tetragonal zirconia polycrystals. *J. Am. Ceram. Soc.*, **73** (1990) 2523–5.
7. Zhang, B., Guo, J. K. & Zhu, P. N., Synthesis of $NaZr_2P_3O_{12}$ powder. *J. Chinese Ceram. Soc.*, **22** (1994) 246–52.
8. Zhang, B., Guo, J. K. & Zhu, P. N., Synthesis and thermal expansion of $M_{1/2}Sr_{1/4}Zr_2P_3O_{12}$ (M = Li, Na, K) compounds. *Ceram. Int.*, **20** (1994) 287–92.
9. Predecki, P., Abuhasan, A. & Barrett, C. S., Residual stress determination in Al_2O_3/SiC whisker composites by X-ray diffraction. *Adv. X-Ray Anal.*, **31** (1988) 231–43.
10. Morishima, H., Kato, Z., Uematsu, K., Saito, K., Yano, T. & Ootsuka, N., Development of aluminum titanate–mullite composite having high thermal shock resistance. *J. Am. Ceram. Soc.*, **69** (1986) C-226–7.
11. Abuhasan, A., Balasingh, C. & Predecki, P., Residual stresses in alumina/silicon carbide whisker composites by X-ray diffraction. *J. Am. Ceram. Soc.*, **73** (1990) 2474–84.
12. Noyan, I. C. & Cohen, J. B., An X-ray diffraction study of the residual stress–strain distribution in shot peened two phase brass. *Mater. Sci. Eng.*, **75** (1985) 179–93.
13. Hoffman, M. Y., Schneider G. A. & Petzow G., The potential of Si_3N_4 for thermal shock applications, in thermal shock and thermal fatigue behavior of advanced ceramics, eds G. A. Schneider & G. Petzow, 1993, Kluwer, Academic Publishers, The Netherlands, pp. 229–44.
14. Becher, P. F., Lewis, III, D., Carman, K R. & Gonzalez, A. C., Thermal shock resistance of ceramics: size and geometry effects in qeunch tests. *Am. Ceram. Soc. Bull.*, **59** (1980) 542–5.